Scientific Contributions Oil & Gas, Vol. 49. No. 2, June: 275 - 295

SCIENTIFIC CONTRIBUTIONS OIL AND GAS

Testing Center for Oil and Gas
LEMIGAS

Journal Homepage:http://journal.lemigas.esdm.go.id
ISSN: 2089-3361, e-ISSN: 2541-0520

Integrated Static–Dynamic Analysis for Sweet Spot Identification and Reserves Prediction in Low-Permeability Reservoirs Using Production Data and Geospatial Attributes

Yuliani Yuniwati[1,2], Dedy Irawan[1], Ivan Kurnia[1], Alfian Gilang[2], and M. Soleh Ibrahim[2]

[1]Petroleum Engineering, Faculty of Mining and Petroleum Engineering, Institut Teknologi Bandung, Ganesa Street No. 10, Bandung, West Java, 40132, Indonesia.

[2]Pertamina EP Zone 4 Regional 1, Jenderal Sudirman Street No. 3, Patih Galung, Prabumulih City, South Sumatra, Indonesia.

Corresponding author: Yuliani Yuniwati (mk.yuliani.liu@pertamina.com)

Manuscript received: February 17th, 2026; Revised: March 26th, 2026
Approved: May 01th, 2026; Available online: June 12th, 2026; Published: June 12th, 2026.

ABSTRACT - The optimization of infill well placement and the reliable prediction of Estimated Ultimate Recovery (EUR) continue to represent critical challenges in low-permeability reservoirs. Conventional permeability evaluation using Pressure Build-Up tests is often impractical due to prolonged shut-in requirements and operational constraints. Although geospatial tools such as Antelope Map effectively identify fracable zones associated with high initial production rates, sustained long-term recovery is not necessarily guaranteed. This study proposes an integrated static–dynamic framework that combines geospatial attributes with production-based analysis to improve reservoirs characterization and well placement decisions. In-situ permeability and flow capacity, expressed as $\sqrt{k}hX_f$, are extracted directly from routine production data of 14 hydraulically fractured wells using the Inverted Decline Curve method, thereby bypassing the limitations of pressure transient analysis. The Stretched Exponential Production Decline model is subsequently applied to generate bounded and realistic EUR predictions. Pearson correlation analysis shows a weak relationship between permeability derived from static logs and EUR. In contrast, the production-derived $\sqrt{k}hX_f$ parameter shows the strongest positive correlation, reflecting effective flow capacity and the influence of matrix heterogeneities such as trace fossils. By comparing the $\sqrt{k}h$ distribution with the static Antelope Map, this dual-criteria approach helps identify sweet spots that support both favorable fracability and more sustained fluid delivery. In general, this data-driven workflow provides a practical alternative framework to reduce geological uncertainty and optimize well placement in low-quality reservoirs.

Keywords: low-permeability reservoirs, sweet spot identification, estimated ultimate recovery, production-based flow capacity analysis, decline curve modeling, static–dynamic integration, geospatial attributes.

How to cite this article:

Yuliani Yuniwati, Dedy Irawan, Ivan Kurnia, Alfian Gilang, and M. Soleh Ibrahim, 2026, Integrated Static–Dynamic Analysis for Sweet Spot Identification and Reserves Prediction in Low-Permeability Reservoirs Using Production Data and Geospatial Attributes, Scientific Contributions Oil and Gas, 49 (2) pp. 275-295. DOI org/10.29017/scog.v49i2.2085.

INTRODUCTION

The sustained growth in global energy demand continues to propel the oil and gas industry toward the development of unconventional and low-permeability reservoirs. In the national context, the Indonesian government has set a strategic production target of one million barrels of oil per day to meet the rising demands of domestic consumption. However, this objective is constrained by the maturity of many producing fields, which are experiencing declining performance due to prolonged high production rates without adequate management of reservoirs. This condition results in premature pressure depletion and low recovery factors, particularly in geologically complex systems.

This challenge according to Sugiantoro (2014) and Widarsono (2013) is evident in South Sumatra, where mature fields still contain significant remaining oil but exhibit low production rates and suboptimal withdrawal performance (0.3–2.4%), showing substantial unrecovered hydrocarbons and limitations of conventional approaches. Consequently, development has shifted toward lower-quality reservoirs, necessitating more advanced and integrated strategies, including optimized well placement and hydraulic fracturing, supported by data-driven integration of dynamic performance data and static geological characterization to enhance recovery efficiency.

Geologically, the primary targets in the KRT Field are located within the Talang Akar Formation (TAF) of the South Sumatra Basin, deposited in a lower shoreface environment. Previous studies (Butarbutar et al., 2023; Gilang et al., 2025) have shown that the performance of reservoirs in highly heterogeneous sandstones is strongly influenced by bioturbation, which modifies pore structure and fluid flow pathways. Petrophysical investigations by Baniak et al. (2015) and Gingras et al. (1999) highlight that trace fossils, such as Glossifungites and Zoophycos, enhance anisotropic permeability by forming secondary micro-flow conduits within otherwise tight matrix systems. These bioturbated intervals establish a dual-porosity and dual-permeability framework, which improves connectivity between the matrix and fracture networks and significantly impacts fluid transport behavior.

From a geospatial perspective, Butarbutar et al. (2023) introduced the Antelope method as a practical approach to identify fracture-prone zones and variations in reservoirs quality. This approach was later applied and further interpreted by Gilang et al. (2025), who emphasized the geological role of bioturbation in shaping sandstone heterogeneity. The study shows that the spatial distribution of bioturbated intervals strongly influences reservoirs quality and fluid flow behavior. These results highlight that the Antelope Map is not only effective in capturing structurally favorable zones but also reflects key geological features that control fracability and production performance.

Gilang et al. (2025) reported a strong correlation between Antelope values and initial liquid production rates, highlighting its effectiveness in predicting early-time productivity and supporting hydraulic fracturing design that can be seen in Figure 1. However, despite its ability to capture favorable geomechanical conditions, this approach remains static and does not fully represent the flow capacity that governs long-term production performance.

While these results confirm the value of geospatial attributes for identifying favorable reservoir zones, they mainly reflect static reservoir characteristics and do not necessarily explain differences in long-term production performance. This limitation suggests the need to integrate production-derived parameters that better represent effective flow capacity and reservoir deliverability over time.

Evaluating the properties of reservoirs in low-quality patterns remains a significant technical challenge due to their complexity, including extreme heterogeneity, fracture–matrix interactions, and prolonged non-linear flow behavior. According to Temizel et al. (2022), Pressure Transient Analysis (PTA) and Rate Transient Analysis (RTA) are widely used diagnostic tools for fracture-dominated systems and are often complemented by Diagnostic Fracture Injection Tests (DFIT) to improve parameter estimation. However, their practical application in tight reservoirs is frequently constrained by operational limitations. PTA requires extended shut-in periods to reach radial flow conditions, RTA is sensitive to fracture complexity and boundary effects, and DFIT introduces additional cost and operational downtime. In the KRT Field, the application of such tests is not feasible due to operational constraints, high costs, and the extremely tight nature of the reservoir, which limits the reliability of the results. As a result, the available dataset is primarily limited to production data and sonolog measurements obtained from the ESP lifting system.

These limitations highlight the need for a practical approach to extract reliable reservoir parameters directly from routine production data as also explained by Hamzah (2021). To address this gap, this study applies the Inverted Decline Curve (IDC) method to estimate in-situ permeability and flow capacity ($\sqrt{k}hX_f$) without requiring well shut-ins, and integrates the results with the Stretched Exponential Production Decline (SEPD) model to generate more realistic EUR predictions.

The IDC method is based on the reciprocal rate formulation introduced by Agarwal, Carter, and Pollock (1979), later applied to fractured gas wells by Chen and Kry (1982) and Neal and Mian (1989) to characterize linear flow behavior. Subsequently, the method is adapted for tight oil reservoirs to estimate their properties and dynamic parameters, including in-situ permeability and productivity index.

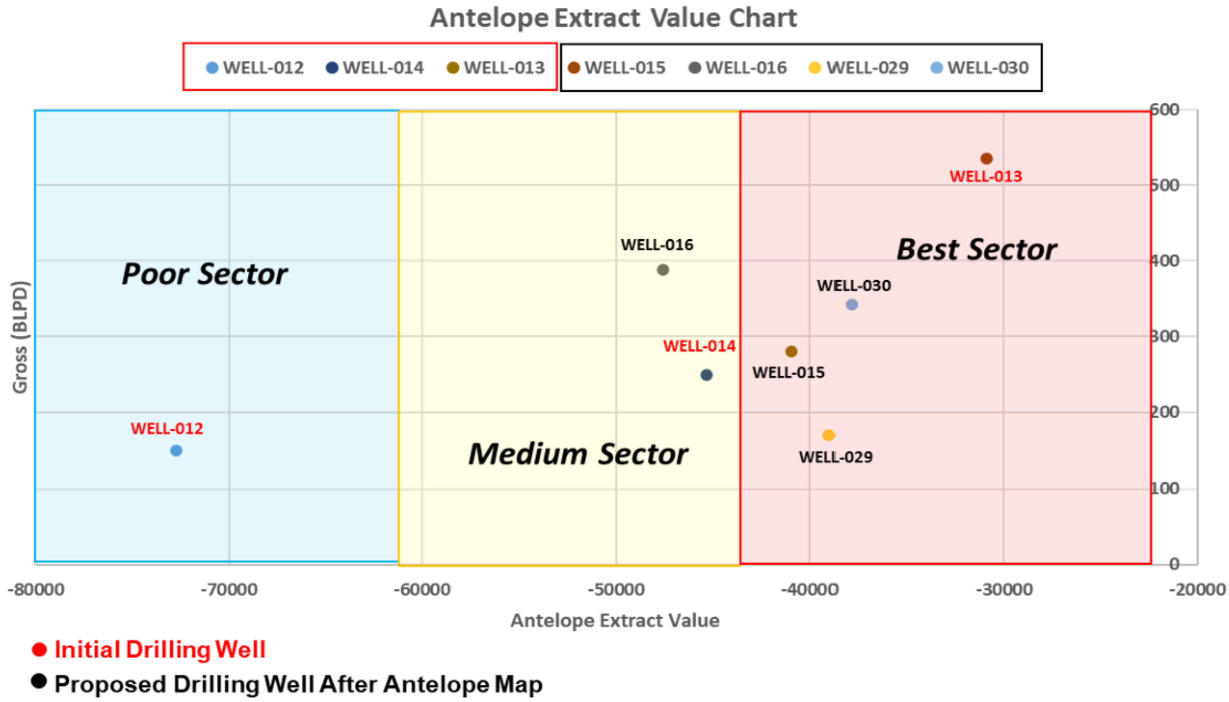

Figure 1. Antelope extract value chart versus liquid production in KRT field (Gilang et al. 2025).

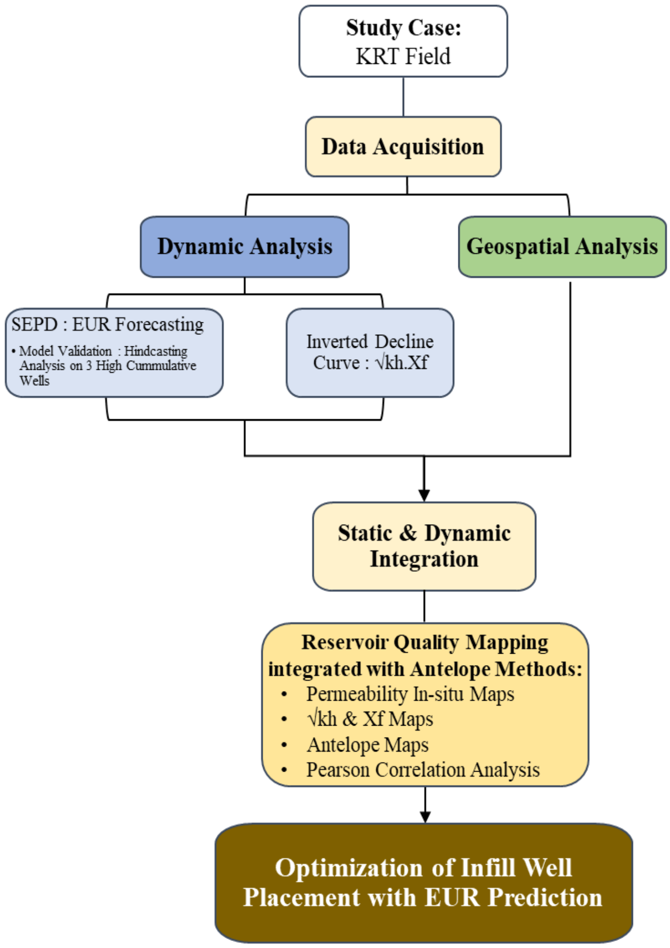

Figure 2. Integrated workflow for infill well optimization and EUR prediction in the KRT field.

The IDC-derived parameters, which exhibit strong correlation with EUR, are integrated with the Antelope Map to support infill well placement. The SEPD model is applied for EUR forecasting and validated through hindcasting against historical production data. In addition, sector-specific EUR regression models are developed to account for heterogeneity in reservoirs and improve prediction accuracy. By linking flow capacity with EUR and integrating it spatially with the Antelope Map, this study establishes a dual-criteria framework that extends beyond initial rate analysis to capture the sustained performance of reservoirs. In general, this integrated approach provides a practical basis for optimizing infill well placement while reducing geological uncertainty in low-permeability reservoirs.

METHODOLOGY

The study methodology is designed as an integrated workflow to optimize infill well placement. This systematic approach is categorized into four primary stages:

- Data acquisition
- Static geospatial analysis
- Diagnostic dynamic analysis
- Static and Dynamic Integration

The comprehensive sequence of this study is shown in the following flow diagram (Figure 2). Figure 2 shows that the workflow begins with the KRT Field as the case study, starting with the data acquisition stage, which includes the collection and quality control of production data, petrophysical data, and geospatial attributes. The analysis is then carried out through two main components: dynamic analysis and geospatial analysis. The dynamic analysis applies the IDC method to extract flow capacity parameters ($\sqrt{k}hX_f$) directly from production data, along with the SEPD model for Estimated Ultimate Recovery (EUR) forecasting. In parallel, geospatial analysis uses seismic attributes, such as Ant-Track and Envelope, to characterize the quality of reservoirs and identify fracture-prone zones.

The results from both analyses are subsequently integrated in the static and dynamic integration stage. This step involves comprehensive quality mapping of reservoirs by combining permeability distribution, flow capacity maps, and Antelope Map, supported by correlation analysis. The integrated interpretation facilitates the identification of sweet spots by incorporating both fracability and long-term flow capacity. Ultimately, this workflow establishes a data-driven framework for optimizing infill well placement and reducing geological uncertainty in low -permeability reservoirs.

Data acquisition and sources

In this study, the dataset used was compiled from multidisciplinary sources, including both subsurface and production data. The primary data consist of historical production records before and after hydraulic fracturing, Post Job Reports (PJR) containing fracture geometry parameters, petrophysical properties derived from well log interpretation (porosity, permeability, net pay, and fluid saturation), and pressure data such as FBHP and WHP. In addition, seismic attributes (Ant-Track and Envelope) and Hydrocarbon Pore Volume (HCPV) Map were used to represent the spatial distribution of reservoir properties.

To accommodate data limitations, analog PVT data from similar formations and core analysis data (RCAL and SCAL) were incorporated to characterize fluid and rock properties. All datasets were subjected to quality control and selection criteria, focusing on wells that have undergone hydraulic fracturing and possess sufficient production history to ensure reliable application of IDC and SEPD analyses.

Time normalization was performed to ensure consistency in production decline analysis by converting calendar time into effective production time, with $t = 0$ defined at the onset of production after hydraulic fracturing, while excluding shut-in and operational interruptions. This approach is essential in low-permeability reservoirs, where extremely low permeability induces pseudo-boundary effects that limit inter-well communication and cause wells to behave as limited drainage systems. Consequently, time normalization minimizes distortion in rate–time relationships, allowing production trends to more accurately reflect intrinsic reservoir behavior and facilitating more reliable flow regime identification and reservoir parameter estimation.

Geospatial analysis

This geospatial methodology has previously been applied in the KRT Field and has been documented in several published conference proceedings (Butarbutar, E.F., 2023; Gilang et al., 2025). Previous implementations have shown the effectiveness of this approach in integrating seismic attributes with reservoir data to support hydraulic fracturing optimization and infill well placement. The positive outcomes from these earlier studies provide a strong foundation for the continued application and further development of this study, particularly in improving the reliability of sweet spot identification and production performance prediction in low-quality reservoirs.

Figure 3 illustrates the workflow used to generate the Antelope Map. The analysis starts with two main datasets: the Hydrocarbon Pore Volume (HCPV) map and the Ant-Track × Envelope seismic attribute map. The HCPV map represents the distribution of hydrocarbon volume within the reservoir, whereas the Ant-Track × Envelope attribute highlights areas associated with fracture development and variations in reservoir quality.

Both maps are then classified into reservoir sectors based on their relative values. The HCPV sectorization distinguishes areas with different levels of hydrocarbon potential, while the Ant-Track × Envelope sectorization identifies zones with varying fracability characteristics. The two

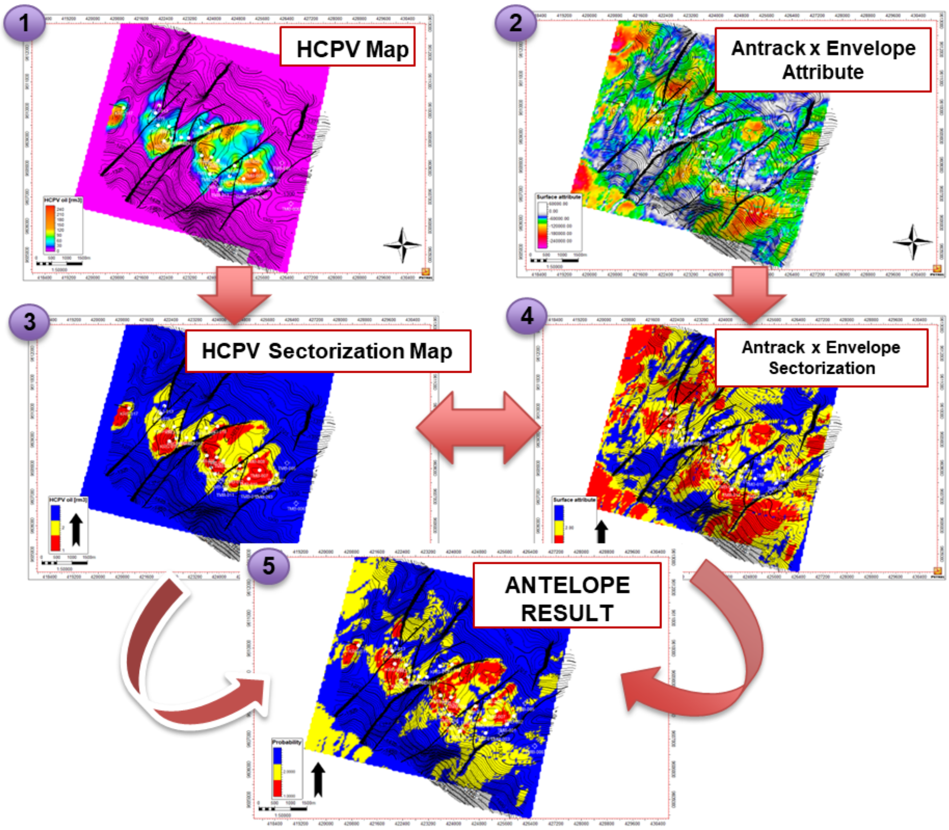

Figure 3. Workflow of Antelope method in mapping visualization (Gilang et al., 2025).

sectorized maps are subsequently combined to generate the Antelope Map, which integrates hydrocarbon potential and reservoir fracability into a single framework. The resulting map is used to identify favorable reservoir areas for hydraulic fracturing and future infill well placement.

In this study, both datasets are standardized through a sectorization process to ensure consistent comparison across maps. In the first step, the seismic attributes, which are Ant-Track and Envelope that combined to generate the Antelope attribute without prior normalization. This approach preserves the original magnitude and variability of each attribute, allowing their combined effect to better represent the characteristics of reservoirs. The resulting Antelope attribute highlights areas where good rock quality coincides with fracture-prone zones. The Antelope value is calculated using a multiplicative relationship:

$$\text{Antelope Value} = \text{Envelope} \times \text{Ant-track}$$

Based on this result, the Antelope Map is further classified using a ranking scheme defined for the KRT Field (Equations 1 and 2)

$$\text{Antelope Rank} = \begin{cases} 3, & \text{if Antelope} > -45{,}000 \\ 2, & \text{if } -95{,}000 \leq \text{Antelope} \leq -45{,}000 \\ 1, & \text{if Antelope} < -95{,}000 \end{cases} \qquad (1)$$

in parallel, the HCPV map is also classified to represent hydrocarbon volume distribution using:

$$\text{HCPV Rank} = \begin{cases} 1, & \text{if HCPV} > 90 \\ 2, & \text{if } 30 \leq \text{HCPV} \leq 90 \\ 3, & \text{if HCPV} < 30 \end{cases} \qquad (2)$$

these two rankings are then integrated through a function:

$$\text{Sector} = f\,(\text{Antelope Rank, HCPV Rank})$$

HCPV values retain volumetric units (e.g., barrels of reservoirs), while Antelope attribute values are dimensionless and represent relative indicators of fracture intensity and quality of reservoirs. Therefore, extracted values from both maps are not directly comparable in magnitude but are integrated through ranking and sectorization for spatial decision-making: 1). This combined classification groups the reservoirs into Best; 2). Medium; and 3). Poor sectors, enabling a more consistent evaluation of quality. By integrating both fracability (from Antelope) and hydrocarbon volume (from HCPV), the method provides a more comprehensive representation of the potential of reservoirs.

The resulting values are extracted along the target horizon using a time-structured surface and mapped to generate the final Antelope Map. Validation at well locations shows a positive relationship with production performance, particularly initial liquid rate (Figure 1). In general, this integrated approach improves the identification of geological sweet spots and supports more reliable infill well placement and hydraulic fracturing optimization (Butarbutar 2023; Gilang et al., 2025).

IDC method

In sequential order, the flow periods in a hydraulically fractured well consist of fracture linear flow, bilinear flow, formation linear flow, and pseudo-radial flow, as shown in Figure 4. Among these flow regimes, the formation linear flow period is particularly important in this study because it forms the basis of the IDC analysis. During this period, the relationship between 1/q and $\sqrt{t}$ becomes linear, allowing reservoir flow capacity and in-situ permeability to be estimated directly from production data.

The evaluation of hydraulically fractured wells under finite-conductivity assumptions was first established by Cinco-Ley et al. (1978), who introduced a mathematical framework and the concept of dimensionless fracture conductivity to describe flow behavior in fractured reservoirs as explained earlier by Gringarten (1974). This work was later validated and extended by Agarwal et al. (1979) through numerical simulations, including constant wellbore pressure solutions and early-time analysis, which are essential for low-permeability systems.

Cinco-Ley and Samaniego (1981) further developed this theory by introducing the concept of bilinear flow, characterized by simultaneous linear flow in the fracture and formation. This regime appears as a constant one-fourth slope (iso-slope) on log–log diagnostic plots, providing a basis for estimating fracture conductivity from early-time pressure data. Thompson (1981) extended these concepts into practical applications using reciprocal rate analysis ($1/q$) showing that production-based methods can effectively describe transient flow behavior in tight reservoirs, where pseudo-steady-state conditions are rarely achieved.

Building on the developments above, Rietman formalized the IDC as a practical tool for analyzing production data, enabling the estimation of permeability, skin, and drainage characteristics. The IDC method relates the reciprocal flow rate to ($1/q$) time functions such as $\sqrt{t}$ or log (t), where characteristic slopes represent different flow regimes. In particular, the linear trend observed during the formation of a linear flow regime provides a practical basis for estimating in-situ permeability and fracture-related parameters under assumptions of high fracture conductivity, minimal wellbore storage, and negligible skin effects.

This behavior is consistent with early-time flow conditions, where fluid flow from the formation toward the fracture is predominantly linear. Under this regime, Chen and Kry (1982) further showed the relationship between gas well production and vertical fractures, assuming a constant bottom-hole pressure during the formation linear flow period, as expressed by the following Equation 3,

$$q_D = {p_{DB}}/{\sqrt{\pi t_D}} \tag{3}$$

where q_D is the dimensionless flow rate, p_{DB} is the dimensionless bottom-hole pressure, t_D is the dimensionless time, and π is a constant.

In this study, this relationship is applied to a tight oil reservoir. The underlying assumptions remain consistent with Chen and Kry (1982), where the bottom-hole pressure is considered constant throughout the linear flow period. This formulation is valid during the linear flow regime, in which fluid flows orthogonally from the formation toward the fracture face. Additional assumptions include a homogeneous reservoir operating under infinite-acting conditions and fully penetrated by a vertical fracture. Under the assumption of constant fluid viscosity and compressibility, the slope can be determined using the following Equation 4,

$$1/q = m\sqrt{t} + s \tag{4}$$

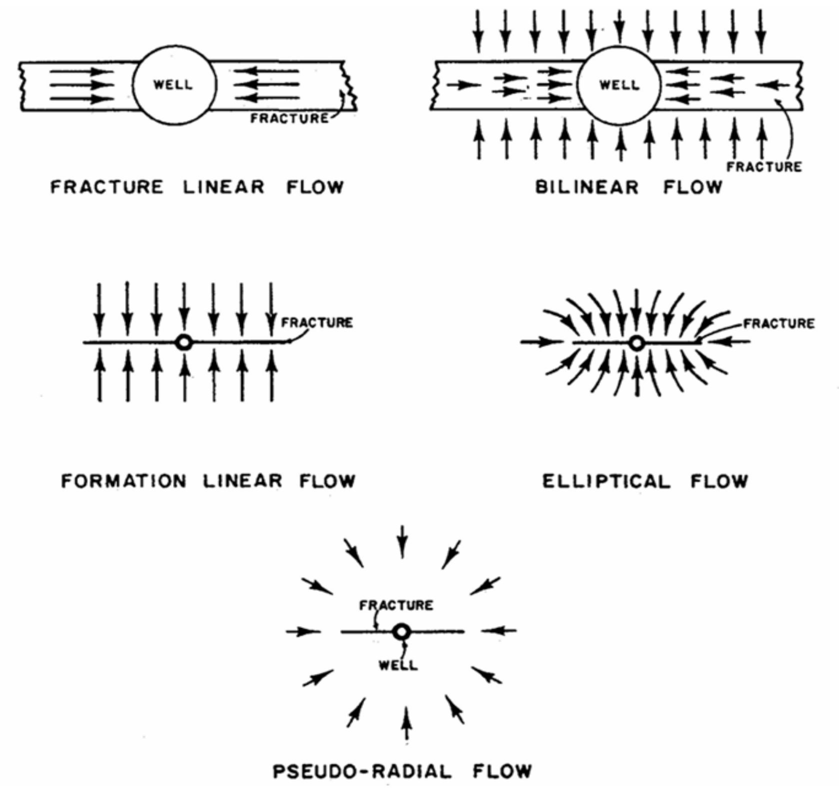

Figure 4. Flow periods in vertically fractured well (Modified by Neal & Mian 1989).

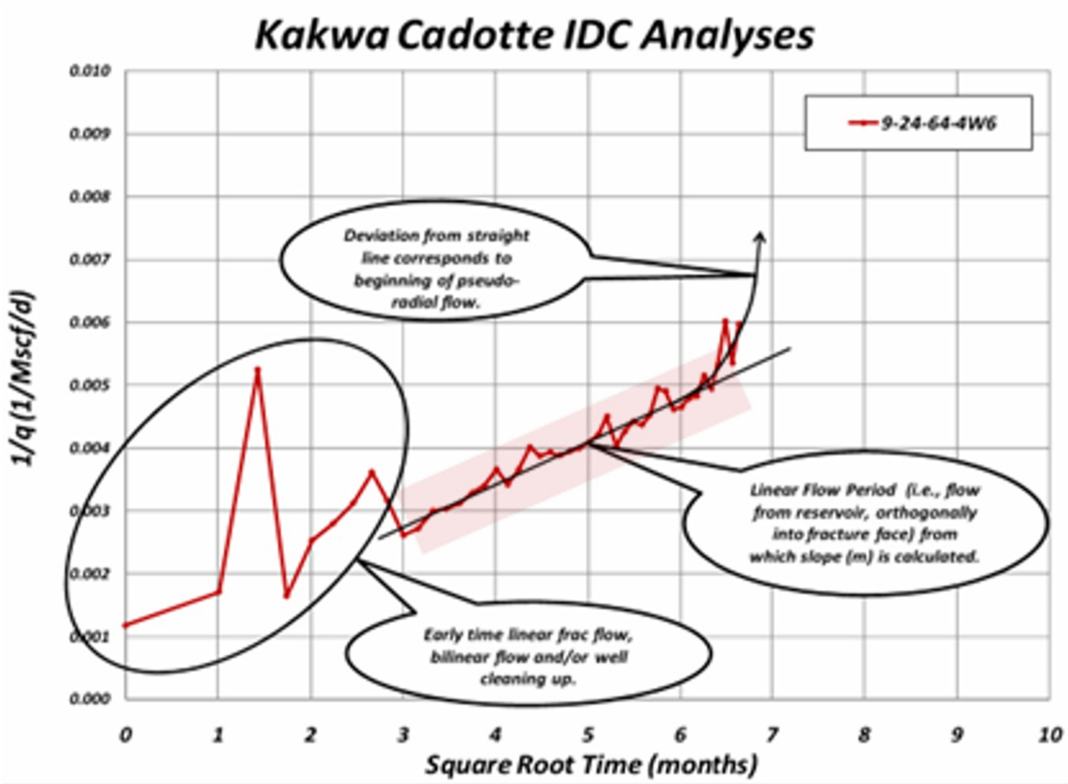

Figure 5. Flow periods in vertically fractured well (Kuppe et al., 2011).

where q is the oil flow rate, t is the production time, m is the slope of the linear flow regime, and s is the intercept.

As shown in Figure 5, the plot of (1/q) versus (√t) exhibits different flow regimes throughout the production period. Early-time data are commonly affected by fracture-dominated flow and well clean -up effects, resulting in scattered responses. A clear linear trend is observed during the formation linear flow regime (highlighted by the transparent red shaded area), where the IDC method is applied to determine the slope used for estimating reservoir flow capacity and in-situ permeability. At later times, the trend begins to curve away from linearity, indicating a change in flow behavior as the reservoir approaches pseudo-radial flow conditions. Agarwal et al. (1979) further described the relationships between dimensionless parameters, such as dimensionless flow rate, (Equation 5)

$$q_D = \frac{141.2\, q_o B_o \mu_o}{2khp_i} \tag{5}$$

where, q_o is the oil production rate (bbl/day), B_o is the oil formation volume factor (bbl/stb), μo is the oil viscosity (cp), k is the permeability (mD), h is the thickness of the reservoirs (ft), and p_i is the initial pressure of reservoirs (psia).

The dimensionless pressure term is expressed as the normalized pressure drawdown relative to the initial reservoir pressure, as shown in Equation 6,

$$p_D = \frac{p_i - p}{p_i} = \frac{\Delta p}{p_i} \tag{6}$$

where p is the flowing bottom-hole pressure (psia), and Δp is the pressure drop (psia).

The dimensionless time term is defined by incorporating the effects of reservoir and fracture properties, as given in Equation 7,

$$t_D = \frac{kt}{\phi \mu c_t x_f^2} \tag{7}$$

where ϕ is porosity (fraction), c_t is total compressibility (psi^{-1}), and x_f is the fracture half-length (ft). Substituting equations 5, 6, and 7 into equation 3 yields the relationship between oil flow rate and fracture half-length. During the linear flow period, the slope (m) can be analyzed, as it contains critical information regarding the fracture length resulting from the fracturing job Equation 8,

$$\frac{1}{q} = \frac{141.2\, B_o\sqrt{\mu_o \pi}}{2h\Delta p x_f \sqrt{k\phi c_t}}\sqrt{t} + s \tag{8}$$

The slope is mathematically defined as Equation 9.1,

$$m = \frac{141.2\, B_o\sqrt{\mu_o \pi}}{2h\Delta p x_f \sqrt{k\phi c_t}} \tag{9.1}$$

For simplification, equation 9.2 is divided into two constants of

$A = 141.2\sqrt{\pi}$

and

$$B = \frac{B_o\sqrt{\mu_o}}{2\sqrt{c_t}\Delta P} \tag{9.2}$$

Based on the reference from Kuppe et al. (2011), A is independent of the well's properties of reservoirs, while B is influenced by the initial conditions of reservoirs. Consequently, the slope equation is simplified to Equation 10,

$$m = AB\left(\frac{1}{\sqrt{k\emptyset} hX_f}\right) \tag{10}$$

where m represents the slope of the linear flow regime, which reflects the fracture and properties of reservoirs. This study shows that the IDC method can be effectively applied to oil wells in the KRT Field and remains reliable even with imperfect production data, as it focuses on the formation linear flow period. The resulting in-situ permeability reflects the effective flow capacity of reservoirs, capturing both matrix and fracture contributions, and is commonly expressed as a composite parameter $\sqrt{k}hX_f$ (Chen & Kry 1982; Neal & Mian 1989). As such, the IDC method provides a more realistic representation of the quality of reservoirs nd serves as a practical tool for identifying zones with favorable flow capacity and fracture characteristics.

SEPD model

Conventional production decline curve analysis, such as the Arps model, is fundamentally inadequate for unconventional and low-permeability reservoirs due to its reliance on pseudo-steady state assumptions as mentioned by Egbe (2023). In tight formations where the transient flow phase is highly prolonged, applying Arps hyperbolic models often yields unrealistic decline exponents (b > 1). To address these complexities, this study uses the SEPD model developed by Valko (2009), which models production decline as a combination of massive, independent, exponentially decaying volumes. Can & Kabir (2012) and Jimenez, et al. (2017) highlight SEPD as the most conservative decline approach, highly favored for generating finite and realistic EUR estimates that inherently mitigate the risk of reserve overestimation. The mathematical formulations for the time-dependent production rate (q_t) and the decline parameter within the SEPD model are defined as Equation 11,

$$q_t = q_o \times e^{-\frac{t^{\beta}}{\tau}} \tag{11}$$

The parameter τ acts as a characteristic time scale (analogous to a half - life), while the dimensionless exponent β dictates the rate and pattern of the decline. One practical advantage of the SEPD model is that its bounded formulation results in a finite EUR, in contrast to the Arps decline model. By establishing a linear relationship between potential hydrocarbon recovery and cumulative production, the SEPD model offers a consistent and robust framework for forecasting long-term performance and estimating EUR in low-permeability reservoirs.

As a comprehensive validation step for the reliability of the SEPD model in estimating EUR, a hindcasting analysis is applied to existing wells with the highest cumulative production (Np) records within each block of reservoirs. This approach partitions the actual historical data into two distinct segments, which include a training period and a validation period. Specifically, the training period is based on 12 to 72 months of actual production from the wells in each block, while the validation period uses 50 to 314 months of actual production data per well. Initially, the τ and β parameters are calibrated exclusively using production data from the training period. The optimized model is subsequently extrapolated forward to forecast continued production trends. The accuracy and robustness of the model are quantitatively evaluated by comparing predicted cumulative production (Np_predicted) with actual cumulative production data (Np_actual) during the validation period. These observed data are deliberately withheld during the calibration process.

Integrated quality of reservoirs and spatial mapping

This integration stage forms the core of the infill well placement framework by seamlessly bridging dynamic well performance with field-scale static geological attributes. Initially, the spatial distribution of $\sqrt{k}hX_f$ parameters from the IDC method are generated using Kriging and Co-Kriging geostatistical approaches. To enhance interpolation accuracy in areas with sparse well control, Co-Kriging integrates high-resolution seismic attributes. Furthermore, these property maps are strictly guided by the NE–SW (N 30°E) regional depositional trends of reservoirs in the TAF formation derived from FMI data, ensuring consistency with the overall geological framework.

Concurrently, static geological properties are represented by the Antelope Map. The resulting map is subsequently constrained by hydrocarbon pore volume (HCPV) to confirm hydrocarbon saturation and normalized on a 0 to 3 scale, using quartile-based geostatistical classification. These ranges are validated against production data to ensure alignment with observed well performance. A spatial comparison between the IDC-derived parameter map and the static Antelope map is conducted to identify sweet spots. Areas exhibiting the intersection of the highest values from both analytical domains are definitely classified as sweet spots. These zones guarantee a combination of favorable mechanical fracability, massive fluid flow capacity, and long-term reserve potential. Through this integrated mapping, the coordinates for proposed infill well placements can be pinpointed precisely, significantly reducing geological and operational uncertainties in low-quality reservoirs.

RESULT AND DISCUSSION

Data pre-processing is conducted to ensure data quality and reliability, as field data often contains noise that may bias subsequent analyses. This stage includes data cleansing to remove nonrepresentative production data such as early clean-up periods, measurement anomalies, surface facility interruptions, and scattered production data caused by artificial lift failures (e.g., ESP or pump malfunction). Time normalization is applied by converting calendar time into effective production time, with t = 0 defined at the onset of post-fracturing production and excluding shut-in periods to maintain continuity in decline analysis.

An example of data pre-processing from Well-09 is shown in Figure 6. The $1/q$ versus $\sqrt{t}$ plot shows a clear linear trend during the formation linear flow regime, showing that production behavior is dominated by fracture-controlled flow. Deviations observed at early time are indicative of clean-up effects, whereas the upward trend at late time suggests a transition toward pseudo-radial flow conditions. The blue-circled region in Figure 6 represents scattered data within the linear flow regime, likely resulting from heterogeneity in reservoirs and operational fluctuations, and is excluded from slope interpretation.

Figure 7 presents representative IDC diagnostic plots for several wells after data pre-processing. Despite differences in production performance and reservoir characteristics, all wells exhibit a distinct linear trend during the formation linear flow regime, indicating that the IDC method can be consistently applied across the study area. The slope of each linear trend varies from well to well, reflecting differences in reservoir flow capacity and fracture effectiveness. These slopes are subsequently used to estimate average in-situ permeability, which represents the effective permeability of the reservoir system by incorporating the combined influence of the matrix and fracture network.

The in-situ permeability values derived from the IDC method are generally higher than those obtained from well log interpretation, as log-derived permeability mainly represents matrix permeability as stated by Musu (2010). This comparison is presented in Figure 8 and highlights the significant role of fracture systems in enhancing flow capacity, with hydraulic fracturing and natural fractures increasing permeability beyond matrix-controlled values.

Despite this enhancement, the overall in-situ permeability values remain relatively limited and highly variable across wells. While this variation fundamentally reflects the extreme reservoirs heterogeneity in the KRT Field, which is dominated by highly bioturbated sandstones, it is also inherently affected by analytical uncertainties. Specifically, the derivation of permeability in the IDC method is sensitive to the slope interpretation during the formation

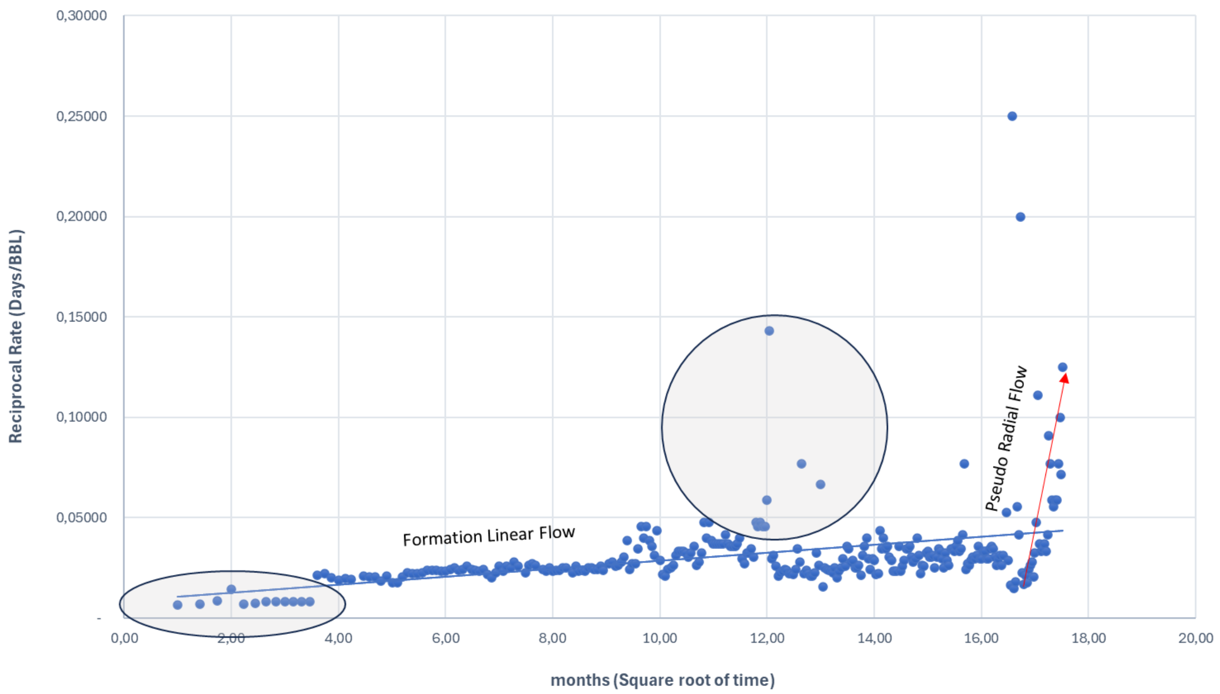

Figure 6. IDC analysis plot for Well-09.

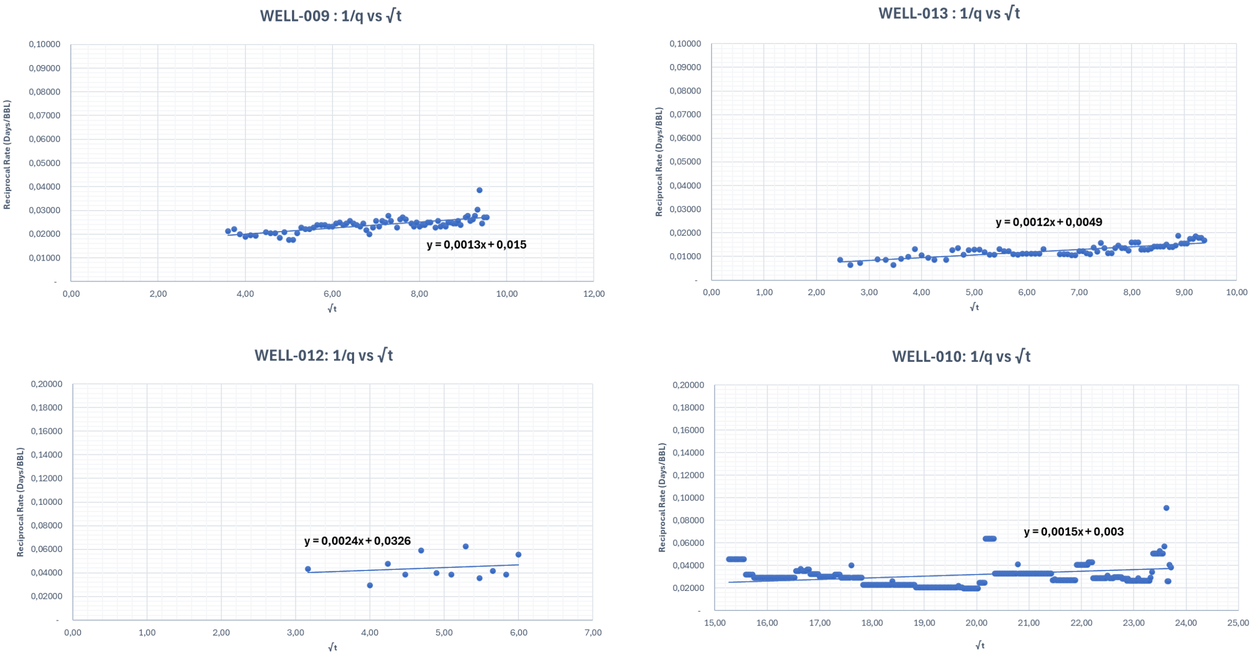

Figure 7. IDC Diagnostic plots (1/q vs √t) for several Wells after pre-processing data.

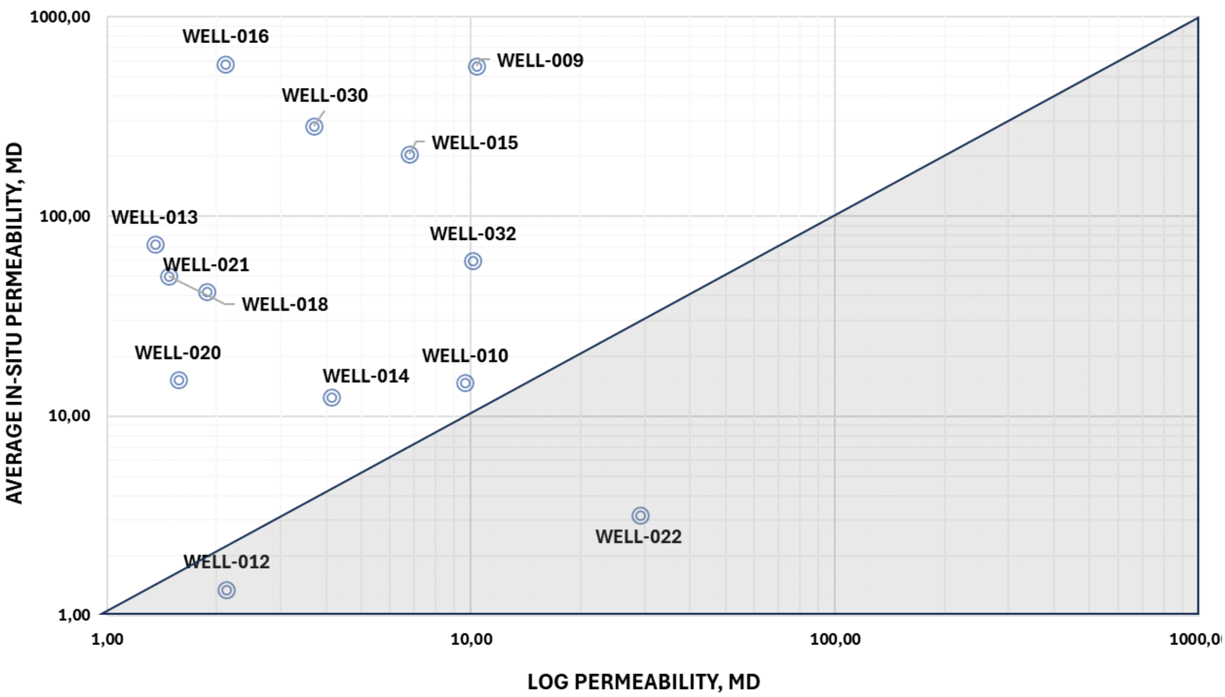

Figure 8. Comparison of IDC-Derived Average In-Situ Permeability and Log-Derived Matrix Permeability.

linear flow regime, as well as the inherent uncertainties associated with the input variables, including average porosity, net pay thickness, and the estimated fracture half-length (Xf).

Although the inherent matrix permeability is low, the successful extraction of high productivity parameters $\sqrt{k}hX_f$ shows that the bioturbated intervals, particularly those enriched with trace fossils such as Glossifungites and Zoophycos, act as preferential flow pathways. Therefore, these intervals form a dual-porosity and dual-permeability system that, when connected to hydraulic fractures, provides sustained fluid flow and defines key sweet spots within reservoirs.

The SEPD model was applied to estimate EUR, with parameters (τ and β) derived from log–log analysis of production data. The hindcasting results, which were applied in 4 wells in each block, show good agreement between predicted and actual production, confirming that SEPD reliably captures long-term behavior. As shown in Figure 9, the model achieves an MAPE of 5.72%, with strong performance for high cumulative wells. SEPD analysis was conducted for all wells in the dataset. However, this study presents only several representative wells, as shown in Figure 10.

The obtained β values show prolonged transient flow typical of low-permeability, heterogeneous reservoirs, thereby highlighting the limitations of conventional Arps models. Besides that, the parameter of τ represents the characteristic time scale controlling production decline, reflecting the combined effect of heterogeneity of reservoirs and flow dynamics. SEPD is considered suitable for EUR estimation and is applied to all wells for further analysis and infill optimization. The EUR estimates for each well, together with the N_p/EUR ratio, are presented in Figure 11.

In Figure 11, The comparison between cumulative production (Np) and EUR shows clear variation in performance across wells in the KRT Field. Some wells, specifically in Block PA (e.g., WELL-009 and WELL-015), have high recovery ratios (>80%), showing that a large portion of reserves has already been produced. In contrast, wells such as WELL-020, WELL-029, and WELL-032 have low recovery (<20%), suggesting they are still in the early production stage and within the transient flow regime. On average, the Np/EUR ratio is approximately 50%, showing that most wells have recovered only about half of their estimated reserves despite having more than 10 months of production history. This result supports the use of the SEPD model, which is appropriate for characterizing long-term production behavior in tight reservoirs.

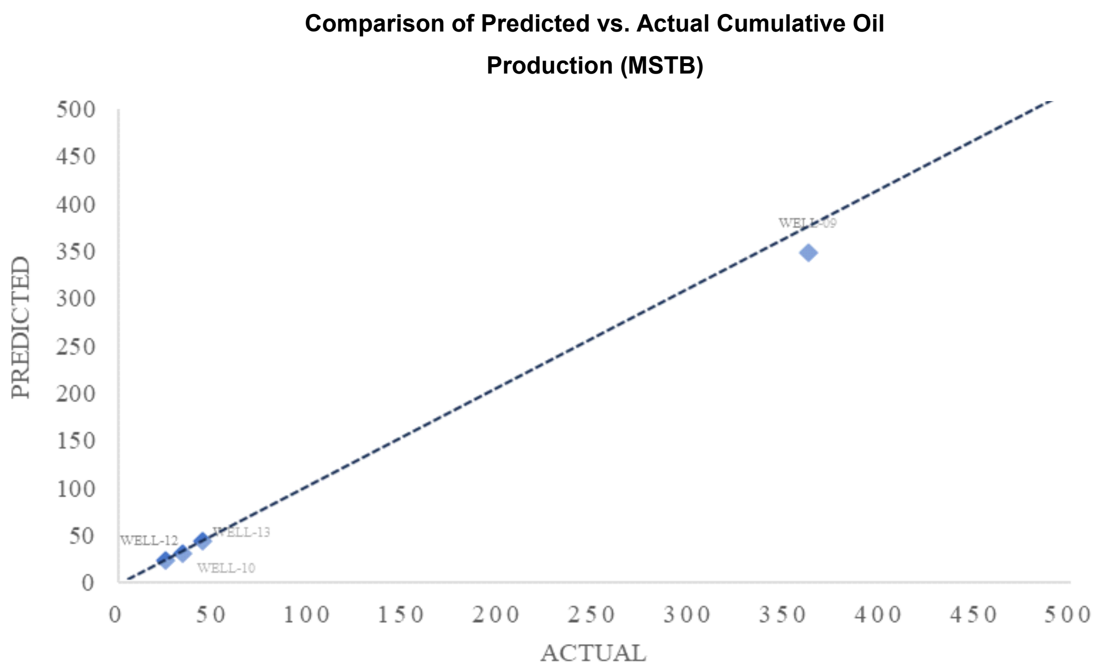

Figure 9. Comparison of Predicted vs Actual Cumulative Oil Production.

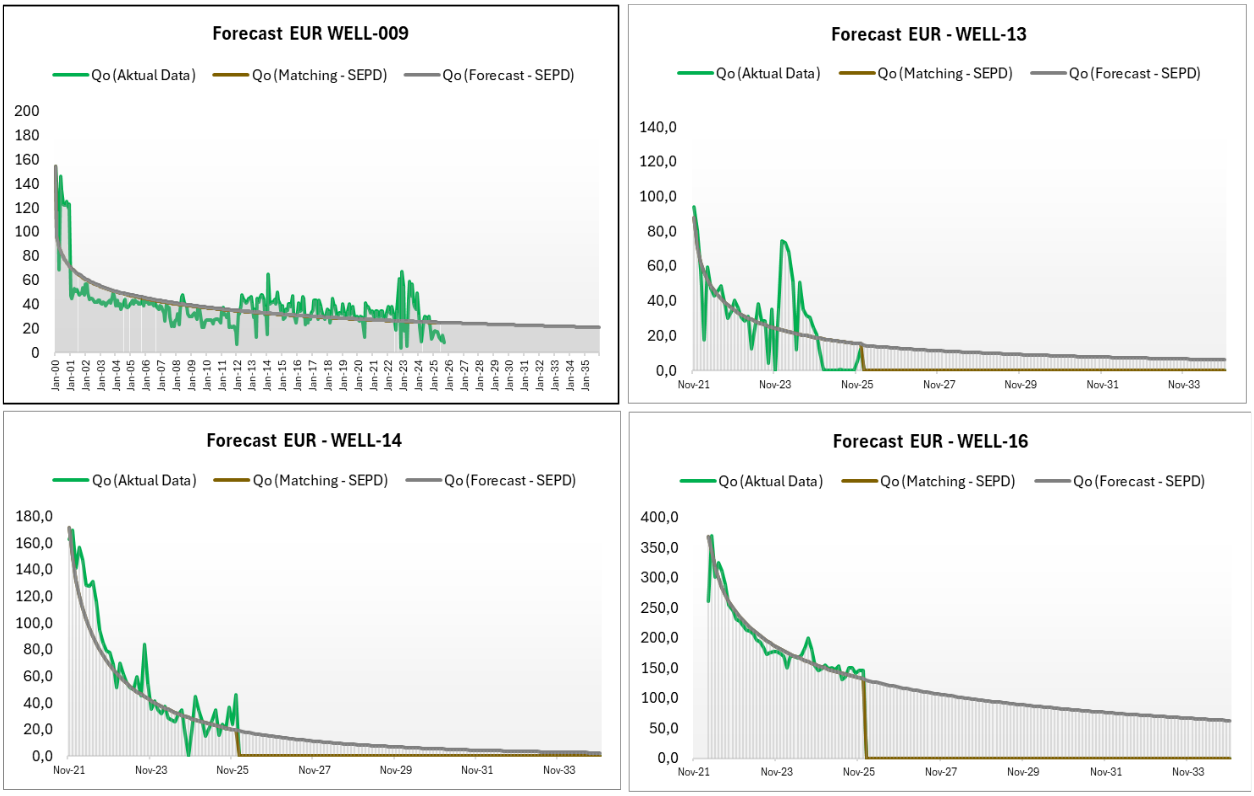

Figure 10. Forecast EUR for several Wells

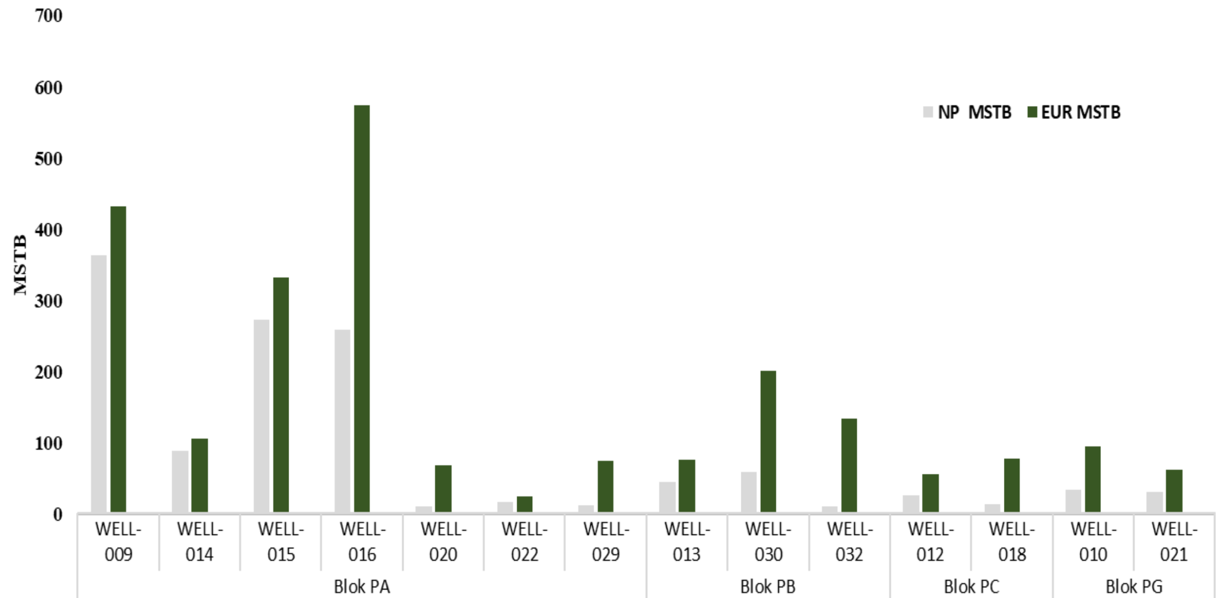

	WELL-009	WELL-014	WELL-015	WELL-016	WELL-020	WELL-022	WELL-029	WELL-013	WELL-030	WELL-032	WELL-012	WELL-018	WELL-010	WELL-021
NP MSTB	362	88	272	259	10	16	12	44	58	10	25	13	34	31
EUR MSTB	432	106	332	575	68	24	74	76	201	133	55	77	95	61
NP/EUR	84%	83%	82%	45%	15%	65%	16%	59%	29%	8%	46%	18%	36%	50%

Figure 11. Comparison of Np, EUR, and recovery Ratio (Np/EUR) Across Wells in the KRT Field.

Parameter	Porosity	Permeability Log	Netpay	FCD	√k.h.Xf	√k.h	Xf	Permeability IDC	Antelope Value	Qoi	τ	β	EUR
Porosity	1,000												
Permeability Log	0,068	1,000											
Netpay	0,556	-0,054	1,000										
FCD	-0,276	-0,193	0,143	1,000									
√k.h.Xf	-0,099	-0,193	0,325	-0,285	1,000								
√k.h	0,068	-0,005	0,491	-0,181	0,754	1,000							
Xf	0,117	-0,119	-0,102	-0,333	0,234	-0,282	1,000						
Permeability IDC	-0,029	-0,043	0,115	-0,261	0,646	0,853	-0,218	1,000					
Antelope Value	0,337	0,045	0,267	-0,545	0,498	0,255	0,345	0,209	1,000				
Qoi	0,129	-0,061	0,396	-0,260	0,865	0,641	0,224	0,516	0,648	1,000			
τ	0,113	-0,324	-0,115	-0,210	0,244	0,270	-0,011	0,367	-0,052	0,015	1,000		
β	-0,110	-0,195	0,043	-0,219	0,471	0,111	0,378	-0,053	0,290	0,384	0,462	1,000	
EUR	0,100	-0,154	0,226	-0,290	0,837	0,736	0,089	0,828	0,501	0,844	0,234	0,102	1,000

-1	-0,5	0	0,5	1

Figure 12. Pearson Correlation Matrix of Properties of Reservoirs, IDC Parameters, and EUR in the KRT Field.

To validate the significance of each variable on the EUR and test the reliability of the proposed framework, Pearson (1920) developed a comprehensive correlation analysis. The evaluated independent variables included static rock parameters (porosity, log permeability, net pay), parameters of reservoirs extracted from the IDC method (in-situ permeability and $\sqrt{k}hX_f$), and spatial index values extracted from the Antelope Map (Antelope Value).

Based on the resulting correlation matrix Figure 12, the correlation matrix highlights a clear difference between the influence of conventional static data and dynamic data. Static rock parameters, such as porosity and log-derived permeability, exhibit very weak, even negative, correlations with EUR (with r values of 0.100 and -0.154, respectively). Net pay also shows only a weak positive correlation (0.226). These results confirm that, in low-permeability reservoirs, both matrix permeability and static formation thickness fail to fully capture actual fluid flow capacity, rendering them inadequate as standalone predictors of long-term production. Strong positive correlations were found in the dynamic parameters extracted using the IDC method. The productivity parameter, $\sqrt{k}hX_f$, recorded one of the highest Pearson correlations with EUR at 0.837. Meanwhile, the extracted Antelope Value also showed a significant positive correlation of 0.501 towards EUR, and a moderately strong correlation of 0.648 towards the initial production rate *(Qoi)*.

Although the Antelope attribute is crucial for delineating structurally and lithologically fracable zones, the influence of $\sqrt{k}hX_f$ is proven to be stronger in controlling EUR. Static seismic attributes (Antelope) do not directly capture post-stimulation flow effectiveness, while $\sqrt{k}hX_f$ provides a direct measurement of the formation's dynamic response. In the KRT Field, the high intensity of bioturbation, specifically the presence of trace fossils, may enhance secondary permeability pathways within the extremely tight rock matrix.

When hydraulic fracturing is applied, the induced fractures effectively intersect and are likely to interact with these trace fossil networks. Consequently, the trace fossils act as micro-flow pathways, significantly facilitating hydrocarbon movement from the tight rock matrix into the main fractures and, in the end, to the wellbore. This complex connectivity and highly effective fluid drainage are mathematically quantified within the value. This mechanism makes it a far superior and more representative EUR predictor compared to purely macroscopic spatial attributes.

Figure 13 shows the spatial distribution of Antelope values across the KRT Field. High Antelope values (red to yellow) indicate areas with more favorable reservoir quality and fracability, while low values (blue) represent less favorable zones. The distribution of these high-value areas generally follows the main structural trends within the field and is associated with several productive wells, supporting the effectiveness of the Antelope Map for identifying favorable fracturing targets.

The integration of the static Antelope Map with the IDC-derived parameter map constitutes the cornerstone of the proposed infill well optimization strategy. As shown by the correlation analysis, the Antelope Map provides a critical spatial framework for delineating highly fracable zones within reservoirs, as shown in Figure 13. Identifying these mechanically favorable areas is important, as these factors facilitate optimal fracture propagation during hydraulic stimulation, thereby yielding improved fracture half-lengths (X_f).

Wells placed in regions with high Antelope Values generally deliver elevated initial production rates (Q_{oi}) due to the extensive initial contact area with reservoirs. However, relying only on fracability to dictate well placement may pose a significant operational risk. Historical field data suggest that wells exhibiting high initial rates may experience rapid production decline if the surrounding formation lacks sufficient fluid-feeding capacity. To mitigate this risk and support long-term production sustainability, the reservoirs property map, specifically the $\sqrt{kh}$ a distribution derived from IDC is introduced as a key tool for enhancing infill well placement.

The $\sqrt{kh}$ map represents areas characterized by high average in-situ permeability, which is shown in Figure 14. The map reveals several localized high-$\sqrt{kh}$ zones (yellow to orange) surrounded by extensive regions of moderate to low values (green to blue), indicating significant spatial variability in reservoir flow capacity across the field. In the context of the highly heterogeneous KRT Field, this in-situ permeability does not only represent the primary matrix permeability, which is inherently tight, but rather reflects an effective average that includes contributions from the tight matrix, induced hydraulic fractures, and secondary permeability networks associated with bioturbation (trace fossils). Higher $\sqrt{kh}$ values show that these combined systems are more effective in draining the matrix and supplying hydrocarbons into the main fractures.

As a result, the final infill well coordinates are selected at the intersection of high Antelope Values and high $\sqrt{kh}$ distributions. This dual-criteria overlay strategy helps reduce the risk of identifying "false prospects" which are zones that may fracture easily but lack sufficient connectivity to sustain flow over time. By targeting these overlapping sweet spots, the proposed infill locations are expected to achieve a strong initial production response (driven by optimized X_f in fracable rock) while maintaining sustained fluid delivery, leading to improved EUR. This integrated workflow reduces geological uncertainty and provides a reliable, data-driven approach for future field development.

Although the proposed workflow exhibits strong predictive potential, several limitations in the available data should be acknowledged. The spatial distribution of the dynamic $\sqrt{k}$ h map is based on only 14 hydraulically fractured wells. Although the analysis is methodologically sound and geologically consistent, this relatively small dataset introduces some level of uncertainty.

In particular, areas with limited well control may be less reliably represented in the spatial

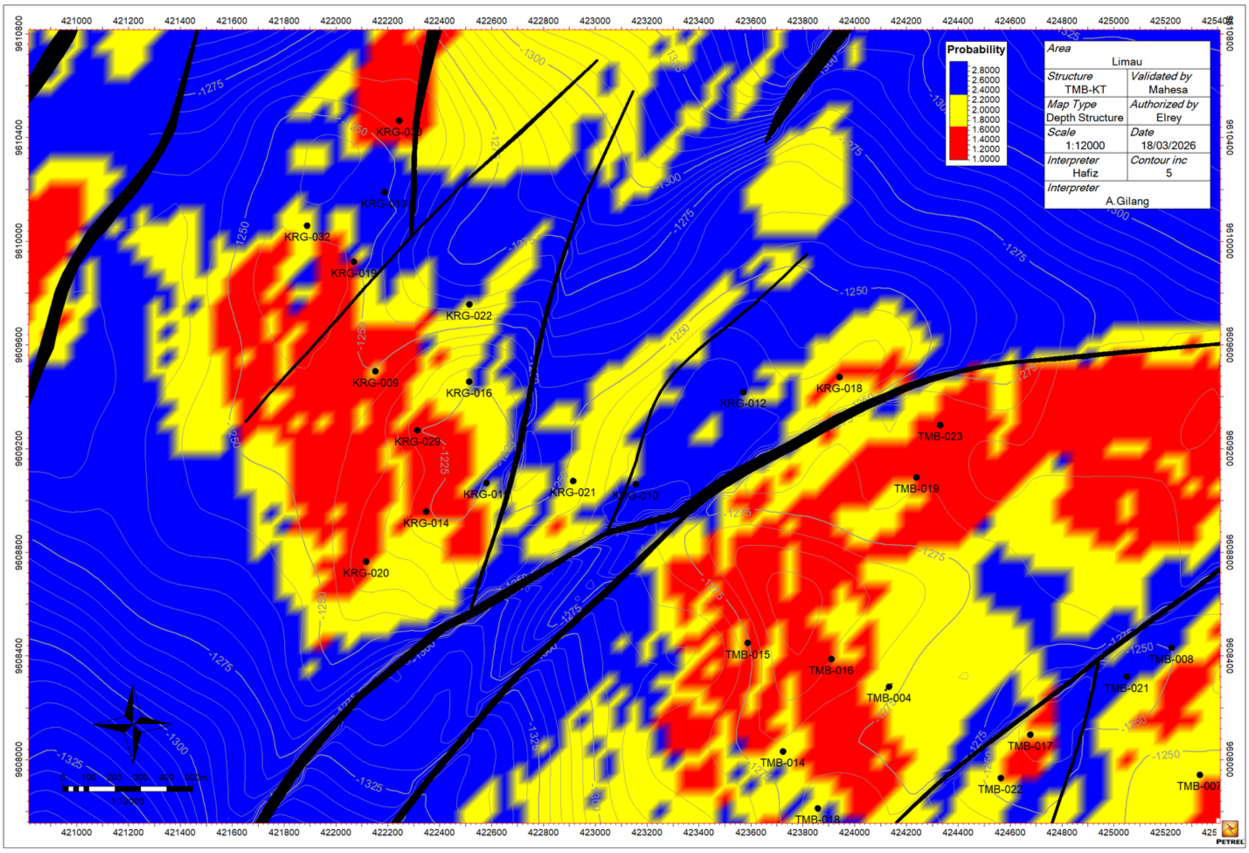

Figure 13. Antelope map in KRT field.

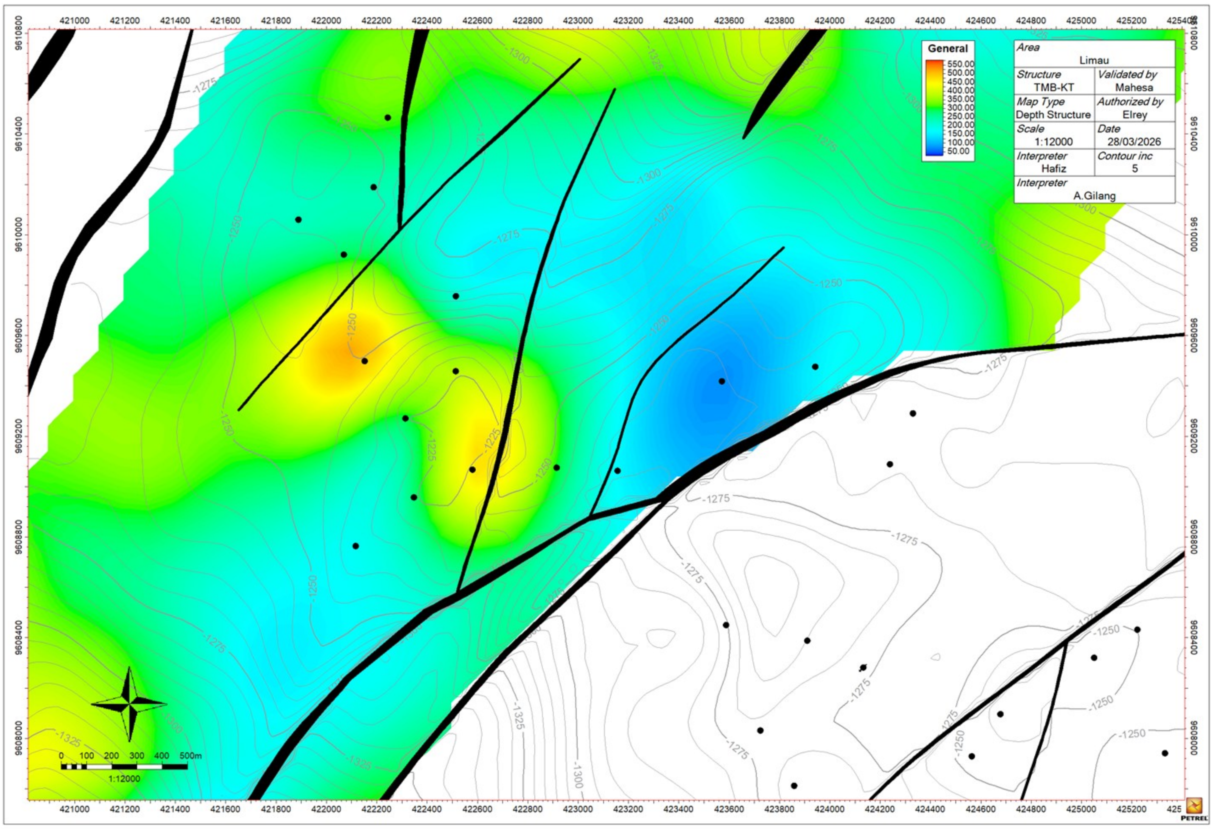

Figure 14. Spatial distribution map of $\sqrt{kh}$ values for the TAF series.

mapping, and the statistical results can be influenced by local variations or outliers. As a result, the identified sweet spots and correlation trends should be viewed as preliminary insights rather than definitive conclusions for the entire field. With the availability of additional data from future infill drilling, the results can be further refined and validated, which is expected to enhance the overall reliability and predictive accuracy of the framework. In general, the results show that combining production-based flow capacity with geospatial data helps identify sweet spots more reliably, not only for strong initial production but also for more stable long-term performance. In the KRT Field, the results are already quite encouraging, suggesting that the workflow captures the key behavior of reservoirs despite the limited data available.

CONCLUSION

In conclusion, based on the integrated analysis of well production performance and static geospatial attributes in the low-permeability KRT Field, this study confirms that the IDC method serves as a reliable and cost-effective alternative for extracting dynamic the properties of reservoirs, including in-situ permeability (k), netpay (h), and Fractured-half length (Xf) directly from production data, this overcome the limitations and high costs associated with conventional Pressure Build-Up (PBU) testing in tight reservoirs.

Correlation analysis using the Pearson method showed that conventional static log parameters, such as porosity and matrix permeability, exhibit weak relationships with well performance, while the dynamic productivity parameter $\sqrt{k}hX_f$ shows the strongest positive correlation with EUR, establishing it as the most reliable predictor variable for long-term recovery. This strong dependency reflects the physical interaction between induced hydraulic fractures and the bioturbated sandstone matrix, where trace fossils generate secondary micro-flow pathways that enhance the connectivity of reservoirs and sustain hydrocarbon flow toward the main fractures. In parallel, the Antelope Map, which is integrating Ant-track and Envelope attributes constrained by HCPV, could prove effective in identifying mechanically favorable zones for hydraulic fracturing, as shown by its moderate correlation with initial production rates and its role in achieving optimal fracture geometry.

Being limited to static attributes may lead to misleading prospect identification, characterized by high initial rates but rapid decline. To mitigate this risk, the integration of static Antelope Map with dynamic IDC-derived $\sqrt{k}h$ maps through spatial overlay enable more reliable delineation of sweet spots that support both effective stimulation and sustained production performance, which overall can reduce uncertainty in infill well placement. For future work, the development of a multivariable empirical regression model for EUR prediction is strongly recommended. Integrating the strong correlations identified in this study, particularly between the properties of reservoirs $\sqrt{k}hX_f$ and the static Antelope index would allow for precise quantitative EUR estimates at any proposed infill location. This continuous development will enhance economic evaluations and support robust decision-making in field management.

ACKNOWLEDGEMENT

The authors wish to thank Pertamina EP Zona 4 for its support and data facilities, which enabled this study to be completed successfully.

DECLARATIONS

Author contribution

Y. Yuniwati performed the data processing, conducted the analysis, developed the methodology, and drafted the manuscript. D. Irawan and I. Kurnia were involved in conceptualization, methodology development, supervision, and reviewed and edited the manuscript. A. Gilang contributed to the geological conceptualization, processed and analyzed the geological data, and assisted in writing the manuscript. M. S. Ibrahim contributed to supervision, data curation, and performed data processing and analysis. All authors read and approved the final version of the paper.

Funding statement

None.

Competing interest

None.

The use AI or AI-assisted technologies

None.

GLOSSARY OF TERMS AND SYMBOLS

Terms & Symbols	Definition	Unit
q	Oil production rate	STB/day
q_i	Initial production rate	STB/day
t	Production time	day
t_n	Normalized production time	day
k	Permeability	mD
h	Net pay thickness	ft
X_f	Fracture half-length	ft
$\sqrt{k}\cdot h\cdot X_f$	reservoir productivity parameter representing flow capacity from the matrix and fracture system	mD^0.5·ft²
ø	Porosity	fraction
c_t	Total compressibility	psi⁻¹
μ	Fluid viscosity	cp
Bo	Oil formation volume factor	bbl/STB
P_i	Initial reservoir pressure	psia
P_{wf}	Flowing bottom-hole pressure	psia
ΔP	Pressure drop (Pi - Pwf)	psi
m	Slope of 1/q vs √t plot during linear flow	-
A, B	Constants in simplified IDC formulation	-
t_D	Dimensionless time	-
q_D	Dimensionless flow rate	-
P_D	Dimensionless pressure	-
τ	Time characteristic	(days/months)
β	Decline exponent	-

REFERENCES

Agarwal, R.G., Carter, R.D., and Pollock, C.B., (1979). Evaluation and Performance Prediction of Low-Permeability Gas Wells Stimulated by Massive Hydraulic Fracturing, SPE 6838. Journal of Petroleum Technology, March 1979, 362–372.

Baniak, G.M., Gingras, M.K., Burns, B.A., Pemberton, S.G. (2015). Petrophysical Characterization of Bioturbated Sandstone Reservoir Facies in the Upper Jurassic Ula Formation, Norwegian North Sea, Europe. Journal of Sedimentary Research, 85, 62–81.

Butarbutar, E.F., Fansuri, T., Suseno, P., Giyatno. (2023). The Relationship Between Envelope x Ant Tracking Seismic Attribute and The Success of Hydraulic Fracturing. Presented at Fifth EAGE Conference on Petroleum Geostatistics, Porto, Portugal, 27–30 November 2023.

Can, B., & Kabir, C.S. (2012). Probabilistic Production Forecasting for Unconventional Reservoirs With Stretched Exponential Production Decline Model. SPE Reservoir Evaluation & Engineering, February 2012, Society of Petroleum Engineers.

Chen, T., dan Kry, R. (1982). Pressure Buildup From a Vertically Fractured Low-Permeability Formation, SPE 9889. Journal of Petroleum Technology, April 1982, 917–924.

Cinco, H., Samaniego, F., and Dominquez, N. (1978). Transient Pressure Behavior for a Well With a Finite-Conductivity Vertical Fracture. SPEJ, 18(4):253–264. SPE 6014.

Egbe, U.C., Awoleke, O.O., Olorode, O.M., & Goddard, S.D. (2023). On the Application of Probabilistic Decline Curve Analysis to Unconventional Reservoirs. SPE Reservoir Evaluation & Engineering, May 2023. Society of Petroleum Engineers.

Gilang, A., Butarbutar, E.F., Soleh I., M., Suseno, P., & Djudjuwanto. (2025). Development Strategy from Low-Quality Reservoirs in Karangan Field, South Sumatra Basin: Insights from Highly Bioturbated Sandstone Analysis. In Proceedings of the 49th Indonesian Petroleum Association Annual Convention & Exhibition, Jakarta.

Gingras, M.K., Pemberton, S.G., Mendoza, C.A., Henk, F. (1999). Assessing the Anisotropic Permeability of Glossifungites Surfaces. Petroleum Geoscience, 5, 349–357.

Gringarten, A.C., Ramey, H.J. Jr., and Raghavan, R. 1974. Unsteady State Pressure Distribution Created by a Well With a Single Infinite Conductivity Vertical Fracture. SPEJ, 14(4):347 –360. SPE 4051; Trans., AIME, 257.

Hamzah, K., Yasutra, A., & Irawan, D. (2021). Prediction of Hydraulic Fractured Well Performance Using Empirical Correlation and Machine Learning. *Scientific Contributions Oil and Gas*, 44(2), 141–152. https://doi.org/10.29017/SCOG.44.2.589.

Jiménez, E.T., Cervantes, R.J., Magnelli, D.E., & Dabrowski, A. (2017). Probabilistic Approach of Advanced Decline Curve Analysis for Tight Gas Reserves Estimation Obtained from Public Data Base. Paper SPE-185556-MS, presented at the SPE Latin America and Caribbean Petroleum Engineering Conference, Buenos Aires, Argentina, 18–19 May 2017.

Kuppe, F., & Carlson, P. (2011). Reservoir Quality Mapping Based on IDC Analyses and Hydraulic Frac Size. Paper CSUG/SPE-149488, presented at the Canadian Unconventional Resources Conference, Calgary, Alberta, 15–17 November 2011.

Musu, J.T., Prasetyo, H. and Widarsono, B. (2010). Integrating Petrography with Core-Log-Well Test Data for Low Permeability Sandstone Reservoir Characterization: Preliminary Recommendation for Production Optimization. LEMIGAS R&D Centre for Oil and Gas Technology, Jakarta.

Neal, D.B., dan Mian, M.A. (1989). Early-Time Tight Gas Production Forecasting Technique Improves Reserves and Reservoir Description, SPE 15432. SPE Formation Evaluation, March 1989, 27–31.

Pearson, K. (1920). Notes on the History of Correlation. Biometrika, 13(1), pp. 25–45.

Rietman, N.D. (1995). Determining Permeability, Skin Effect and Drainage Area from the Inverted Decline Curve IDC, SPE 29464. Paper presented at the Production Operations Symposium, Oklahoma City, OK, U.S.A., 2–4 April 1995.

Sharma, S., Ali, A.M., Pandey, S., Sharma, L., Aggarwal, A., Jha, A., Gondalia, R., Suyal, S., Shah, B., Joshi, P., Satyanarayana, A., Shaikh, M. & Raman, R. (2020). Unconventional Tight Sand Oil: Breaking the Evaluation Barriers. Offshore Technology Conference Asia, OTC-30173-MS.

Sugiantoro, J.J. (2014). Analisis Laju Pengurasan Produksi Minyak Lapangan-Lapangan Sumatera Selatan. Lembaran Publikasi Minyak dan Gas Bumi (LPMGB), Vol. 48, No. 3, pp. 133–140. https://doi.org/10.29017/LPMGB.48.3.1219.

Temizel, C., Canbaz, C.H., Palabiyik, Y., Hosgor, F.B., Atayev, H., Ozyurtkan, M.H., Aydin, H., Yurukcu, M., & Boppana, N. (2022). A Review of Hydraulic Fracturing and Latest Developments in Unconventional Reservoirs. Paper OTC-31942-MS, presented at the Offshore Technology Conference, Houston, TX, USA, 2–5 May 2022.

Thompson, J.K. (1981). Use of Constant Pressure, Finite Capacity Type Curves for Performance Prediction of Fractured Wells in Low Permeability Reservoirs. Paper SPE 9839 presented at the 1981 SPE/DOE Joint Symposium on Low Permeability Gas Reservoirs, Denver, 27–29 May 1981.

Valkó, P.P. (2009). Assigning Value to Stimulation in the Barnett Shale: A Simultaneous Analysis of 7000 Plus Production Histories and Well Completion Records. Paper SPE 119369 presented at the SPE Hydraulic Fracturing Technology Conference, The Woodlands, Texas, USA, 19–21 January 2009. Society of Petroleum Engineers.

Widarsono, B. (2013). Cadangan dan Produksi Gas Bumi Nasional: Sebuah Analisis atas Potensi dan Tantangannya. *Lembaran Publikasi Minyak dan Gas Bumi (LPMGB)*, Vol. 47, No. 3, pp. 115–126. https://doi.org/10.29017/LPMGB.47.3.244